Title

Mammographic Variation Measures, Breast Density, and Breast Cancer Risk.

Journal

American Journal of Roentgenology, 217(2)

ISSN

0361-803X

Authors

Heine, John
Fowler, Erin
Scott, Christopher G
et al.

Publication Date

2021-08-01

DOI

10.2214/ajr.20.22794

Peer reviewed

HHS Public Access

Author manuscript

AJR Am J Roentgenol. Author manuscript; available in PMC 2022 August 01.

Published in final edited form as:

AJR Am J Roentgenol. 2021 August ; 217(2): 326–335. doi:10.2214/AJR.20.22794.

Mammographic Variation Measures, Breast Density and Breast Cancer Risk

John Heine[1], **Erin Fowler**[1], **Christopher G. Scott**[2], **Matthew R. Jensen**[2], **John Shepherd**[3], **Carrie B. Hruska**[2], **Stacey J. Winham**[2], **Kathleen R. Brandt**[2], **Fang F. Wu**[2], **Aaron D. Norman**[2], **Vernon S. Pankratz**[4], **Diana L. Miglioretti**[5,6], **Karla Kerlikowske**[*,7], **Celine M. Vachon**[*,†,2]

[1]Moffitt Cancer Center, Tampa, FL.

[2]Mayo Clinic, Rochester, MN.

[3]University of Hawaii, Honolulu, HI.

[4]University of New Mexico Health Sciences Center, Albuquerque, NM.

[5]University of California, Davis, Davis, CA.

[6]Kaiser Permanente Washington Health Research Institute, Seattle, WA.

[7]University of California, San Francisco, San Francisco, CA.

Abstract

OBJECTIVE.—Our previous work showed variation measures, representing breast architecture derived from mammograms, were significantly associated with breast cancer. For replication purposes, we examined the association of three variation measures, V measured in the image domain and P_1 and p_1 from restricted regions in the Fourier domain, with breast cancer risk in an independent population. We also compared these measures to volumetric density measures, percent density and dense volume, from a commercial product.

[†]**Corresponding Author:** Please address correspondence to Celine M. Vachon; vachon.celine@mayo.edu; Mayo Clinic, 200 First Street SW, Rochester, MN 55905.

[*]Joint senior authors

Contributions of Authors

This multi-center study involved three teams that designed the study, compiled the case-control samples at two institutions, including using electronic and abstracted data, retrieved and processed images, assessed density measures, analyzed variation, performed statistical analyses and drafted and reviewed the papers. Specific contributions are by author initials below.

Funding for the study (CMV, KK)
Designed the study (CMV, KK, VSP, DLM)
Complied case-control samples, using electronic and abstracted means (CGS, MRJ, VSP, DLM, SJW, JS, KK, CMV)
Identification, retrieval, processing of images (CGS, JS, CGS, KRB, FFW)
Assessed volumetric density measures (JS, FFW, KRB)
Analyzed variation measures (EF, JH)
Critical technical expertise of mammogram measures (CH)
Statistical analyses (CGS, MRJ, DLM, SJM, VSP)
Drafted paper (JH, EF, KK, CMV, CH)
Reviewed and contributed to submitted draft (all authors)
Overall study management (AN)

IRB Statement

Each study was approved by the relevant institutional review board and was compliant with the Health Insurance Portability and Accountability Act.

MATERIALS AND METHODS.—We examined 514 breast cancer cases and 1377 controls from a screening practice, matched for age, race, exam date, and mammography unit. Spearman's rank order correlation was used to evaluate the monotonic association between measures. Breast cancer associations were estimated using conditional logistic regression, adjusted for age and body mass index. Odds ratios were calculated per standard deviation increase in mammographic measure.

RESULTS.—These variation measures were strongly correlated with volumetric percent density (correlations 0.68 to 0.80) but not dense volume (correlations 0.31 to 0.48). Similar to previous findings, all variation measures were significantly associated with breast cancer [odds ratios per standard deviation (95% confidence intervals)]: 1.30 (1.16, 1.46) for V; 1.55 (1.35, 1.77) for P_1; 1.51 (1.33, 1.72) for p_1. Associations of volumetric density measures with breast cancer were similar [1.54 (1.33, 1.78) for percent density; 1.34 (1.20, 1.50) for dense volume]. When including dense volume with each variation measure in the same model, all measures retained significance.

CONCLUSION.—These variations measures were significantly associated with breast cancer risk, comparable to the volumetric density measures, but independent of the dense volume.

Introduction

Mammographic breast density is a significant breast cancer risk factor usually estimated from two-dimensional (2D) mammograms with various methods [1–6]. Breast density measures most often capture the degree or amount of dense tissue on a mammogram [7], as exemplified by the percentage of breast density measure [1]. However, mammographic texture has also shown significant association with breast cancer [4, 8–10]. The earliest example of mammographic texture was a four-category parenchymal pattern classification (i.e. Wolfe's parenchymal patterns), which combined structure and radiographic density [11, 12].

Texture measurements can be derived with various techniques such as filtering (Laws or wavelet filters), run length analyses, and co-occurrence measures [9]. Evidence indicates that texture and breast density both contribute to predicting future breast cancer incidence [13]. Texture features, then, may provide complementary information to breast cancer risk. Texture analysis was recently used to categorize the breast into four distinct radiomic phenotypes, which were independent of breast density [14]. Texture features, then, may provide complementary information to breast cancer risk and a greater understanding of molecular mechanisms relating breast parenchyma with risk.

In this report, we evaluated three related generalized automated mammographic measures. We refer to these as generalized [15] because they do not quantify dense tissue directly. Two of these measures are related and derived in the Fourier domain, referred to as P_1 and p_1 (a normalized version of P_1). Each measure can be considered as a component from the respective set of measures that decompose the power spectrum of a given mammogram non-parametrically in a radial spatial frequency coordinate system, described below. This technique was developed earlier to compare the spectra of mammograms in different data formats [16] and was subsequently evaluated for breast cancer risk with both digitized film [9] and full field digital mammography (FFDM) [15] images. The third generalized measure is referred to as V (for variation), calculated as the standard deviation of the pixels within

the breast area. Previously, V was significantly associated with breast cancer in studies that used both FFDM [17] and digitized film [18] images. In this current study, we examined the association of these generalized measures with breast cancer within two screening practices to replicate our previous findings in different breast screening settings. We also compared these measures with Volpara™ measures [19], volumetric breast density (VBD) and dense volume (DV), which are used in clinical practice [20], and were shown previously to be associated with breast cancer risk [21–23] (Volpara version 1.5.3; Matakina Technology, Wellington, New Zealand).

Materials and Methods

Study Population

We used a case-control study described previously [21] to evaluate the associations of five mammographic measures (i.e., P_1, p_1, V, VBD and DV) with breast cancer. This study was nested within the Mayo Clinic breast screening practice, Rochester, Minnesota; these data were collected from women in a large Midwestern screening practice. This study was approved by the relevant institutional review board and was compliant with the Health Insurance Portability and Accountability Act. It included 514 breast cancer cases with approximately three matched control subjects (N = 1377) without prior breast cancer. Controls were matched to each case on age, race, FFDM examination date, unit, facility, and state of residence. Mammograms were acquired with Hologic Selenia (Hologic, Inc., Bedford, MA) FFDM units (i.e., units that only acquire standard two-dimensional mammograms), which use direct x-ray detection. Raw images were used for this study. These have 70μm pitch with 14 bit dynamic range per pixel. The generalized measures were restricted to the cranial-caudal (CC) views to avoid chest wall interference.

For generalization purposes, we also examined these measures in a second case-control study with 1474 cases and 2942 controls matched controls, also described previously [21–23]. This study was derived from the San Francisco Mammography Registry (SFMR) in Northern California. SFMR participates in the National Cancer Institute-funded Breast Cancer Surveillance Consortium (BCSC) (http://www.bcsc-research.org/index.html). Unlike the primary study, mammograms from this study were not archived in raw image format. Raw images were reduced in resolution to140μm pitch with a lossy (irreversible) compression technique to decrease data size for storage purposes. Images were up-sampled to their native pixel dimensions for the processing in this report.

Variation Measures of Breast Density

Fourier measures: This is a general approach, described in detail previously [15, 16]. The power spectrum of a given mammogram is summarized into a set of n measurements (defined as $P = [P_1, P_2, P_3 \ldots P_m]$), where the set size is adjustable with m = n-1. The spectrum is divided into n concentric rings (bands). The sum over the i^{th} ring produces P_i (i =1 to m, referred to as the ring analysis); note, the P_0 measure is not included in the set. To apply Fourier analysis to mammograms, we first automatically determined the largest rectangle that fits within the breast area [15] illustrated in Figure 1. We take the Fourier transform (FT) of this region and form the power spectrum followed by the summary

analysis, which produces P. Figure 2 shows the basic ring scheme in the Fourier domain using coarse ring-width illustration. In this example, n = 6 and the highest resolvable spatial frequency component is defined as f_c measured in cycles/mm, which gives a radial ring width of $\Delta = f_c/6$ cycles/mm. Summarizing the power in each ring gives 5 different measurements. The regions exterior to the rings can be summarized as another measure (i.e. the corners). The related measure, p_i, is normalized at the image level: $p_i = P_i/$ (total power from the set of the rings + the power in the corners for a given woman). On the mammography units used in the study, detector pitch = 0.07mm, giving fc ≈ 7.14 cycles/mm based on the Nyquist relationship [24, 25]. In this report, we restricted the analysis to P_1 and p_1 (derived with n = 86) due to related work with images acquired with the same type of FFDM units [16]. These two measures are constrained to this radial spatial frequency range: 0.0833–0.166 cycles/mm corresponding with radial spatial precocities between 6–12mm. A given measure can also be viewed as a texture metric. The related texture can be derived by taking the FT of the raw image, discarding the entire Fourier domain signal except for the portion contained in a specified ring followed by Fourier inversion.

Variation measure in the image domain: V was calculated as the standard deviation of the pixel values within an eroded breast area. If we consider the breast area as a semicircle, this area was eroded inward radially by 25% and 35% (i.e., the new radius was either 0.75×original radius or 0.65×orginal radius, respectively) to reduce unwanted variation. This produced two variants of V that were analyzed separately. The erosion process results in a coarse estimation of the area corresponding to where the breast was *uniformly* compressed during the image acquisition. The two variants of V produced similar findings [data not shown]. Therefore, we discussed the variant derived with 65% erosion in our results.

Relationship between the variation measures: Both V and P capture variation and are related. The set of measures within P decompose V. Summing the components of P (including the corners and the center providing the region in the image domain was mean centered) gives V^2 when considering the same mammographic region; this relationship follows from the well-known Fourier power conservation relationship between the image and Fourier domains. This relationship is an approximation in our application because it does not account for the influences of the related pre-processing [16] and that we used different regions with considerable overlap (i.e., the rectangular region compared to the eroded breast region).

Generalized measures and texture: The generalized measures tend to be abstract when describing breast density. As such, we have provided examples of these measures relative to visible image characteristics. The information captured by the Fourier measures can be interpreted as texture when viewed in the image domain. Mammograms shown in Figure 1 (top row) correspond with high and low values of P_1. Mammograms in the bottom row of Figure 1 have more central P_1 values. Figure 3 shows the associated texture captured by P_1 (or p_1) for the mammograms in the top row of Figure 1. Note, the first ring measure captures longer-range (i.e., coarse) image structure. These examples (Figure 1 and Figure 3) also illustrate the difficulty in attempting to untangle the connection between the variation

measures and breast density. In Figure 3, the image on the left (relatively large P_1) has varied regions comprised of both adipose and dense tissue, whereas the image on the right (relatively low P_1 value) tends to be more homogenous comprised of primary adipose tissue. The image on the left (Figure 3) also has increased V due to its spatial variability. In contrast, visually both images appear to have a very similar underlying coarse structure as indicated in Figure 3.

Volumetric breast density: Volpara™ (*Version 1.5.3*, Matakina Technology Limited, Wellington, New Zealand), an automated methodology for assessing volumetric breast density from raw FFDM images with a proprietary algorithm, was used in this study [20]. This assessment is based on estimating the compressed breast thickness, determining image areas of absolute adipose tissue, and considering the x-ray attenuation of breast tissue [26]. We considered both the volume of fibro-glandular tissue volume (DV) measured in cm^3 and volumetric breast density (VBD), the ratio of DV to total breast volume.

Statistical Analyses

Risk factor distributions are presented by breast cancer status. Spearman's rank order correlation (ρ) was used to evaluate the monotonic association between the various breast density measures based on the control distributions. For each measure, the average of the measurements taken from the left and right CC views was used as the mammographic feature metric. Associations of the mammographic measures with breast cancer were evaluated using conditional logistic regression, adjusted for study, age, and body mass index (BMI). We used odds ratio (OR) with 95% confidence intervals (CIs) as the primary metric to evaluate and compare the association of various image measurements with breast cancer. An OR derived from a case-control study from a given population can be used as an approximation for the relative risk for the same population when the disease incidence is small. Odds ratios were estimated for continuous [per standard deviation (SD) increment] measures and measures based on quartiles, both derived from the control distribution. In the continuous model, an OR=1.x is interpreted as a x% increase in risk relative to an individual with a measurement that is one SD less than this specific measurement under evaluation. The second quartile was used as the reference in the quartile models. The area under the receiver operator characteristic curve (Az) was calculated with 95% CIs to summarize the discriminatory ability of the models. A second set of associations were investigated while adjusting for DV, which was not strongly correlated with other mammographic measures. Statistical analyses were performed in the SAS (SAS Institute, Cary, NC) environment with version 9.4. Image analyses were performed in the IDL (Harris Geospatial Solutions, Boulder, CO) environment with version 8.6.

Results

The study characteristics are shown in Table 1. Cases and controls were similar in racial composition [primarily Caucasian (> 98%)], age, BMI and menopausal status but from two different screening populations (Midwest vs. west coast). Parity and age of first birth showed relatively small variations (about 3%) across groups. In contrast, cases were more likely to have a family history of breast cancer. For all breast density measures except p_1, the mean

was greater for cases. Similarly, the case group had a greater proportion of women in the BI-RADS 4 category, whereas controls had a greater proportion of women in the BI-RADS 1 category. The second screening study had greater proportions of younger women, women of Asian ancestry, high breast density (BI-RADS 4), nulliparous women but lower BMI (data not shown) [21–23]. Differences between the two studies are likely due to regional demographical variations.

The five mammographic measures exhibited varying degrees of correlation (referenced as ρ) ranging from 0.30 to 0.95 as shown in Table 2. As expected, the two Fourier measures were strongly correlated with $\rho = 0.95$. These measures showed moderate correlation with V: $\rho = 0.68$ with p_1, and $\rho = 0.74$ with P_1. VBD showed similar correlation with the three generalized variation measures: $\rho = 0.68$ with V, $\rho = 0.82$ with p_1, $\rho = 0.80$ with P_1. In contrast, correlation between DV with the generalized variation measures and VBD was weaker: $\rho = 0.48$ with V, $\rho = 0.31$ with p_1, $\rho = 0.33$ with P_1, and $\rho = 0.30$ with DV.

All continuous mammographic measures showed significant associations with breast cancer (Table 3, Model a). These ranged from OR=1.30 for V (Az=0.59) to OR=1.55 for P_1 (Az=0.61). Similar results were observed when examining quartiles of mammographic measures with breast cancer risk (Model b) for quartiles three and four versus the second quartile reference.

Due to the weak correlation between DV and the other measures, we considered a third model for each of the other four mammographic measures while controlling for DV (Table 3, Model c). ORs were slightly attenuated compared with their respective continuous measure (Model a) but remained significant; Az showed minimal to no gain with the addition of DV.

Associations between mammographic measures and breast cancer were similar in the second screening study, even with the differences in image format (Table 4).

Discussion

We compared five mammographic measures that can be broadly grouped into two classes: VBD and DV capture dense tissue volume directly, whereas the variation measures capture structure in the mammogram and are related to density. The generalized variation measures, V, P_1 and p_1, showed moderate correlation with VBD and weak correlation with DV. All mammographic measures showed similar associations with breast cancer in both the primary and secondary studies. When controlling for DV, the associations for the three generalized breast density measures with breast cancer were attenuated but remained significant, indicating these measures are independent of DV.

The Fourier measures can be described as texture features. These measures have perfect frequency domain localization due to the sharp and infinitely steep separation between the rings. These measures are defined precisely over a spatial frequency range, which is related to the corresponding spatial periodicity range and specific texture range. The tradeoff for this Fourier domain localization is poor spatial localization. Most often, texture features derived from filtering split the difference between frequency and spatial localization. In

contrast with the Fourier metrics, V is a broad-band measure containing the entire Fourier spectrum, containing all spatial scales and image textures. In our analysis, localization was not an issue because each measure corresponds to the entire breast area (or region of interest) and can be considered as a global metric. In contrast with global metrics, other researchers argue that a localized measurement approach may be more useful [10]. As noted, many studies have investigated texture methods using mammograms as outlined in these review articles [4, 8]. Often the focus of texture work is multivariate in character [10, 13, 27, 28], where the precise description of a given feature is not the study focal point [10], in contrast to our work with the Fourier measures in this report.

These generalized mammographic measures have been shown to translate across various settings. The specific Fourier measures showed significant associations with breast cancer previously when evaluating images acquired with both indirect and direct x-ray detection FFDM technologies [16]. These prior findings along with those in this report are also in agreement with our related work with digitized film [9]. Similarly, V has shown to be associated with breast cancer across populations and imaging platforms [17, 18]. This general agreement indicates these measures are capturing reproducible characteristics related to breast structure. Although both P_1 and p_1 are related, the p_1 measure is normalized at the individual level and may be the preferred measure when merging data from many sources. In sum, the work shows that variation is associated with breast cancer, confirming our earlier findings.

There is an important connection between V and P_1 worth comment. The spectral shape of mammograms is well approximated as an inverse power law [16, 29]; when obeying this form, the image domain variance is influenced heavily by the lower spatial frequencies. Theoretically, the power is infinite as the spatial frequencies tend to zero. It follows that the value of V in a given image is strongly dependent upon the lower spatial frequencies in particular the strength of P_1 as indicated by their strong correlation.

A reproducible automated measure of breast density could provide clinical utility for both risk prediction and as an indicator of mammographic performance, such as the BI-RADS composition descriptors. First, there is consensus that risk based breast screening strategies would be beneficial to optimize detection while minimalizing harms associated with mammography [30]. Although inclusion of breast density in risk modeling improved prediction accuracy in multiple studies, overall discrimination accuracy was still limited [31]. The most appropriate method of incorporating image measurements in risk modeling remains a work in progress. In this study, we replicated prior studies showing the variation measures as breast cancer risk factors in two independent studies. These metrics are potential candidates as image measurements for incorporation into risk modeling because they are reproducible and result from relatively simple algorithm without determining thresholds or other parameters related to the image acquisition. Second, these measures may be relevant for characterizing mammographic performance. Because the generalized measures do not provide an output that can be interpreted as breast density directly, their translation to clinical applications may require additional processing steps. One method would be to combine these measures with another breast density measure such as DV in a joint modeling approach for risk prediction. However, our findings did not suggest these

two measures together improved discrimination of risk. Previous work [32] showed how to convert continuous measures, such as V, to both a BI-RADS like breast composition measure and a four state ordinal measure for risk prediction. Our correlation findings suggest that regression analysis could also be used to map a given generalized measure to the range of an accepted standard measure of breast density.

This study has several limitations worth noting. For the variation measures, portions of the breast area were excluded from the analysis and only included mammograms in the CC orientation were considered. In many instances, the excluded area was considerable (up to 35%) due to the erosion process, but we still found strong associations. In the second study, mammograms were evaluated that were missing high frequency information relative to the raw images. Mammograms have a predominantly low-frequency characteristic (i.e. the missing high frequency information accounts for a small fraction of the image variance). Our reproducibility of findings by the second study showed that these measures are robust to the high frequency information and population characteristics. Further, our analyses did not formally evaluate the contribution of these measures to known breast risk models. Given the modest associations and similarity to breast density estimates, however, it is not likely they will significantly change the Az for risk.

Conclusion

In summary, we investigated two generalized methods of measuring variation in mammograms for risk prediction and made comparisons with measures that capture dense tissue. V is a broadband metric whereas the Fourier measures are restricted. These measures have shown association with breast cancer over multiple studies and imaging platforms. The breast cancer associations with these generalized measures were similar to those produced by the volumetric density measures. The specific scale properties of the Fourier measures may be useful for informing other studies examining the biological aspects of breast density. Future work includes investigating interval versus screen-detected cancers with these measures. Whether these measures are useful in clinical applications will require further investigation.

Acknowledgements

Supported by grants R01CA177150, R01CA166269, and U01CA200464 from the National Institutes of Health.

References

1. Boyd NF, Martin LJ, Bronskill M, Yaffe MJ, Duric N, Minkin S. Breast tissue composition and susceptibility to breast cancer. J Natl Cancer Inst 2010; 102:1224–1237 [PubMed: 20616353]
2. McCormack VA, dos Santos Silva I. Breast density and parenchymal patterns as markers of breast cancer risk: a meta-analysis. Cancer Epidemiol Biomarkers Prev 2006; 15:1159–1169 [PubMed: 16775176]
3. Pettersson A, Graff RE, Ursin G, et al. Mammographic density phenotypes and risk of breast cancer: a meta-analysis. J Natl Cancer Inst 2014; 106
4. He W, Juette A, Denton ERE, Oliver A, Marti R, Zwiggelaar R. A Review on Automatic Mammographic Density and Parenchymal Segmentation. Int J Breast Cancer 2015; 2015:276217 [PubMed: 26171249]

5. Bond-Smith D, Stone J. Methodological Challenges and Updated Findings from a Meta-analysis of the Association between Mammographic Density and Breast Cancer. Cancer epidemiology, biomarkers & prevention : a publication of the American Association for Cancer Research, cosponsored by the American Society of Preventive Oncology 2019; 28:22–31
6. Eriksson M, Li J, Leifland K, Czene K, Hall P. A comprehensive tool for measuring mammographic density changes over time. Breast cancer research and treatment 2018; 169:371–379 [PubMed: 29392583]
7. Destounis S, Arieno A, Morgan R, Roberts C, Chan A. Qualitative Versus Quantitative Mammographic Breast Density Assessment: Applications for the US and Abroad. Diagnostics (Basel) 2017; 7
8. Gastounioti A, Conant EF, Kontos D. Beyond breast density: a review on the advancing role of parenchymal texture analysis in breast cancer risk assessment. Breast Cancer Research 2016; 18:91 [PubMed: 27645219]
9. Manduca A, Carston MJ, Heine JJ, et al. Texture features from mammographic images and risk of breast cancer. Cancer Epidemiol Biomarkers Prev 2009; 18:837–845 [PubMed: 19258482]
10. Zheng Y, Keller BM, Ray S, et al. Parenchymal texture analysis in digital mammography: A fully automated pipeline for breast cancer risk assessment. Medical physics 2015; 42:4149–4160 [PubMed: 26133615]
11. Wolfe JN. Breast patterns as an index of risk for developing breast cancer. AJR American journal of roentgenology 1976; 126:1130–1137 [PubMed: 179369]
12. Wolfe JN. Risk for breast cancer development determined by mammographic parenchymal pattern. Cancer 1976; 37:2486–2492 [PubMed: 1260729]
13. Wanders JOP, van Gils CH, Karssemeijer N, et al. The combined effect of mammographic texture and density on breast cancer risk: a cohort study. Breast Cancer Res 2018; 20:36 [PubMed: 29720220]
14. Kontos D, Winham SJ, Oustimov A, et al. Radiomic Phenotypes of Mammographic Parenchymal Complexity: Toward Augmenting Breast Density in Breast Cancer Risk Assessment. Radiology 2019; 290:41–49 [PubMed: 30375931]
15. Fowler EEE, Smallwood A, Miltich C, Drukteinis J, Sellers TA, Heine J. Generalized breast density metrics. Physics in Medicine and Biology 2019; 64
16. Heine JJ, Velthuizen RP. Spectral analysis of full field digital mammography data. Med Phys 2002; 29:647–661 [PubMed: 12033559]
17. Heine JJ, Fowler EEE, Flowers CI. Full field digital mammography and breast density: comparison of calibrated and noncalibrated measurements. Academic radiology 2011; 18:1430–1436 [PubMed: 21971260]
18. Heine JJ, Scott CG, Sellers TA, et al. A novel automated mammographic density measure and breast cancer risk. J Natl Cancer Inst 2012; 104:1028–1037 [PubMed: 22761274]
19. Solutions V. Volpara density user manual version 1.5 Wellington, New Zealand: Volpara Solutions from Matakina Technology 2013;
20. Volpara. Volpara Density User Manual Version 1.5.11 Wellington, New Zealand: Volpara Solutions, 2013. Volpara Solutions from Matakina Technology
21. Brandt KR, Scott CG, Ma L, et al. Comparison of Clinical and Automated Breast Density Measurements: Implications for Risk Prediction and Supplemental Screening. Radiology 2016; 279:710–719 [PubMed: 26694052]
22. Kerlikowske K, Scott CG, Mahmoudzadeh AP, et al. Automated and Clinical Breast Imaging Reporting and Data System Density Measures Predict Risk for Screen-Detected and Interval Cancers: A Case–Control Study. Ann Intern Med 2018; 168:757–765 [PubMed: 29710124]
23. Kerlikowske K, Ma L, Scott CG, et al. Combining quantitative and qualitative breast density measures to assess breast cancer risk. Breast Cancer Research 2017; 19:97 [PubMed: 28830497]
24. Bracewell RN. Two-dimensional imaging Englewood Cliffs, N.J.: Prentice Hall, 1995:xiv, 689 p.
25. Brigham EO. The fast Fourier transform and its applications Englewood Cliffs, N.J.: Prentice Hall, 1988:xvi, 448 p.

26. Highnam R, Sauber N, Destounis S, Harvey J, McDonald D. Breast Density into Clinical Practice In: Maidment ADA, Bakic PR, Gavenonis S, eds. 11th International Workshop of Digital Mammography. Philadelphia, PA: Springer 2012:466–473

27. Nielsen M, Vachon CM, Scott CG, et al. Mammographic texture resemblance generalizes as an independent risk factor for breast cancer. Breast Cancer Res 2014; 16:R37 [PubMed: 24713478]

28. Wang C, Brentnall AR, Cuzick J, Harkness EF, Evans DG, Astley S. A novel and fully automated mammographic texture analysis for risk prediction: results from two case-control studies. Breast Cancer Res 2017; 19:114 [PubMed: 29047382]

29. Heine JJ, Deans SR, Velthuizen RP, Clarke LP. On the statistical nature of mammograms. Medical physics 1999; 26:2254–2265 [PubMed: 10587206]

30. Bitencourt AG, Rossi Saccarelli C, Kuhl C, Morris EA. Breast cancer screening in average-risk women: towards personalized screening. The British journal of radiology 2019; 92:20190660 [PubMed: 31538501]

31. Vilmun BM, Vejborg I, Lynge E, et al. Impact of adding breast density to breast cancer risk models: A systematic review. European journal of radiology 2020; 127:109019 [PubMed: 32361308]

32. Fowler EE, Sellers TA, Lu B, Heine JJ. Breast Imaging Reporting and Data System (BI-RADS) breast composition descriptors: automated measurement development for full field digital mammography. Med Phys 2013; 40:113502 [PubMed: 24320473]

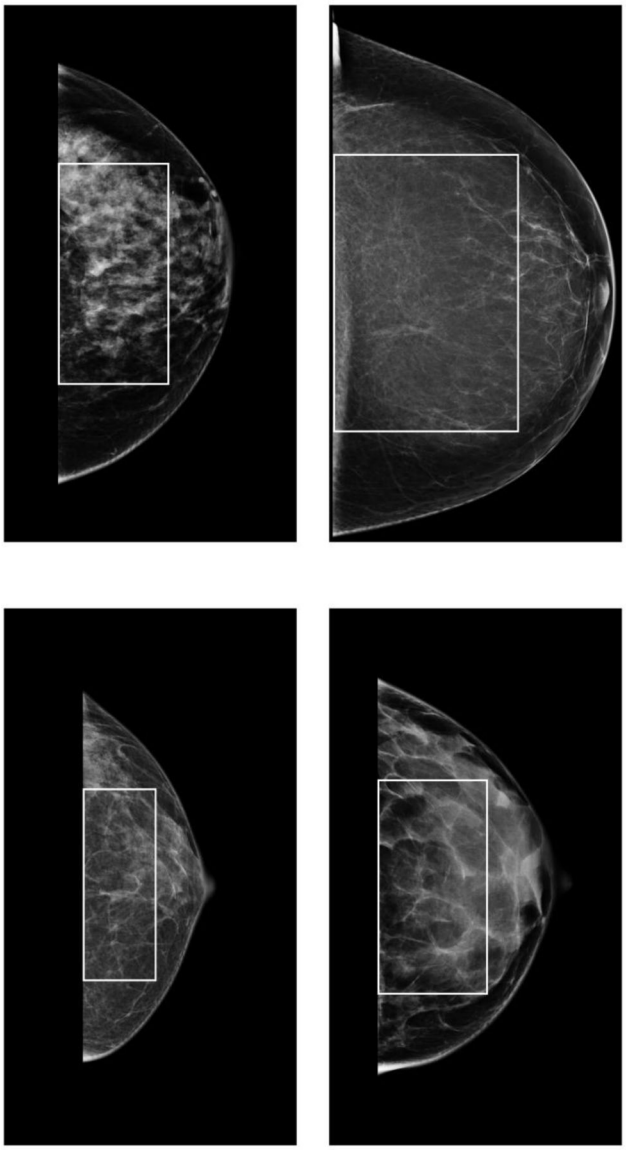

Fig. 1—. Mammogram Illustrations:

This shows four clinical display mammograms on (for presentation format used for viewing purposes only) with the rectangular regions of interest outlined. The mammogram in the top left (1.a) has a pronounced breast density pattern and large P_1 value (75.0), whereas the mammogram on the top right (1.b) tends to have a more adipose characteristic with a low P_1 value (1.4). The top-row illustrations (1.a and 1.b) were selected specifically. The mammograms in the bottom row were selected at random and tend have typical breast density patterns. The image on the bottom left (1.c) and bottom right (1.d) have more central P_1 values (19.4 and 13.8 respectively). Fourier analysis was constrained to these regions.

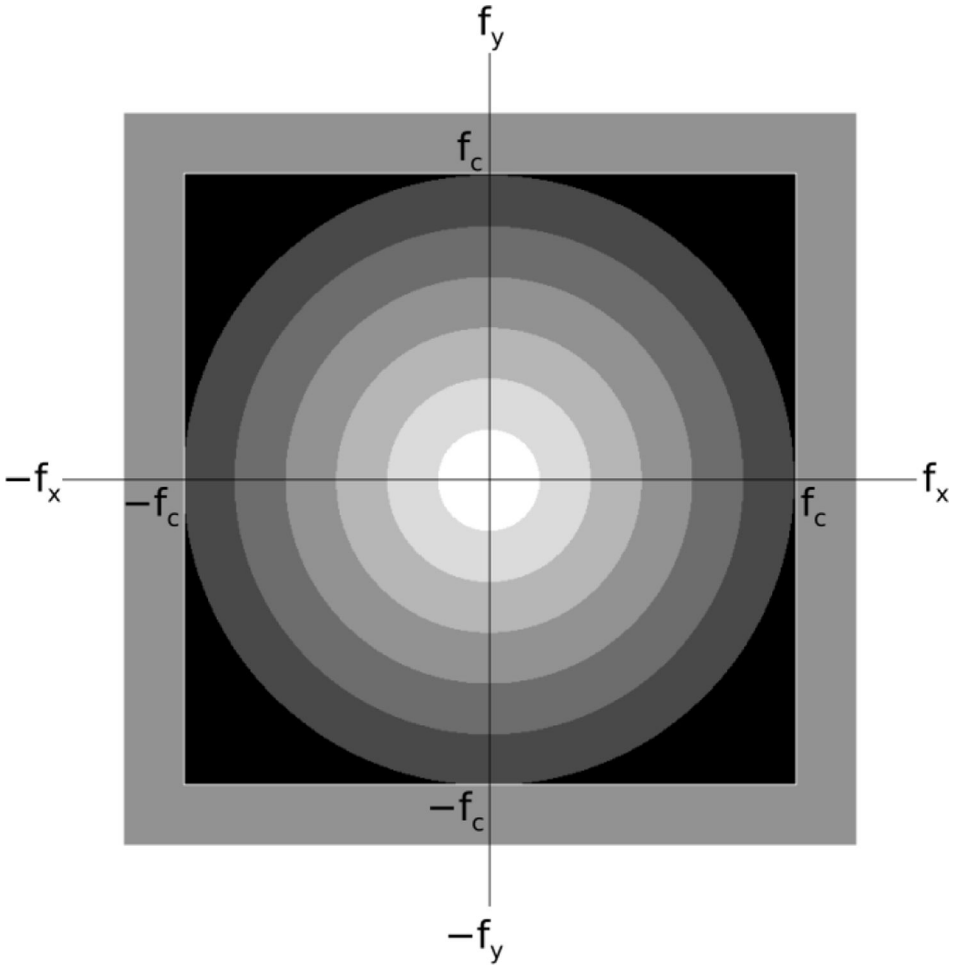

Fig. 2—. Fourier ring measurement illustration:

This shows the Fourier domain overlay (mask) or a coarse ring-width example. This overly is centered in the Fourier Domain. The zero frequency coordinate, (f_x , f_y) = (0, 0) is in the center , where f_x an f_y are Cartesian spatial frequency domain coordinates. There are 5 rings plus the center giving n = 6. The highest resolvable spatial frequency component is defined as f_c. The coordinates of the SE, NE, NW, and SW corners are (-f_c, f_c), (f_c, f_c), (-f_c, f_c) and (-f_c, -f_c), respectively. Ring widths are given by f_c/6 in a radial direction. In this numbering scheme, the center (white-disk) corresponds to m = 0 and the outer ring with m = n-1, where m is the ring index. This mask is used as an overlay for the power spectrum, where the sum over each ring produces a measure. The outer portion (dark regions) of the spectrum not included within the rings is referred to as the corners and can be used as an additional measure.

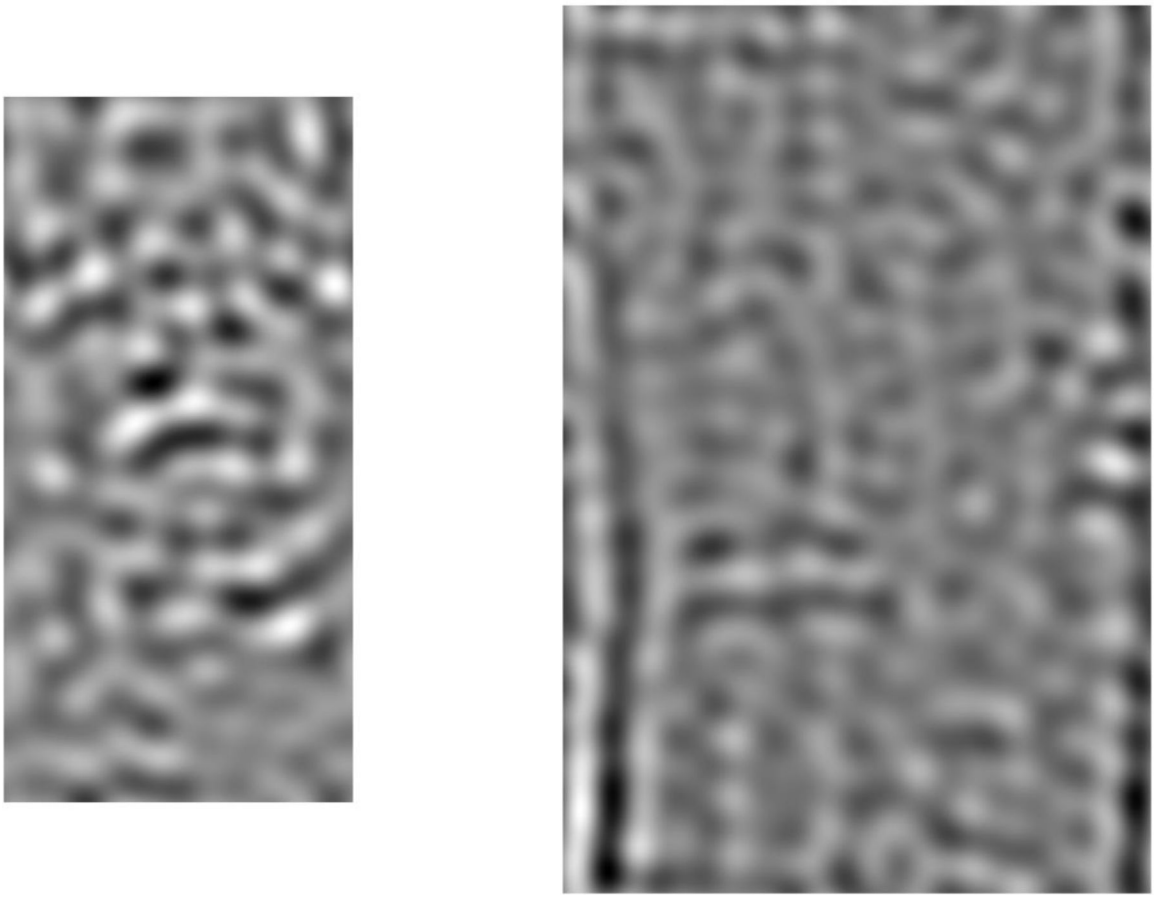

Fig. 3—. Texture Captured by P_1:

These show the structure captured by the first ring corresponding to the mammogram sections shown in the top row of Figure 1. The region on the left (3.a) corresponds with Figure 1.a and the region on the right (3.b) corresponds with Figure 1.b.

Table 1.

Study Characteristics

Population Characteristics						
Measure	**Case n**	**Case Mean (standard deviation) or relative frequency**	**Control n**	**Control Mean (standard deviation) or relative frequency**	**Total n**	**Total Mean (standard deviation) or relative frequency**
Age at Mammogram	514	61.7 (11.4)	1377	61.6 (11.1)	1891	61.6 (11.2)
Race						
Caucasian	505	98.4%	1366	99.4%	1871	99.2%
Asian	4	0.8%	2	0.1%	6	0.3%
Other	4	0.8%	6	0.4%	10	0.5%
Unknown	1	-	3	-	4	-
BIRADS						
1	81	15.8%	340	24.7%	421	22.3%
2	208	40.5%	586	42.6%	794	42.0%
3	188	36.6%	384	27.9%	572	30.2%
4	37	7.2%	67	4.9%	104	5.5%
BMI	483	28.9 (6.3)	1346	28.7 (6.3)	1829	28.7 (6.3)
1st Degree Family History of Breast Cancer						
No History	360	70.3%	1075	78.1%	1435	76.0%
History	152	29.7%	301	21.9%	453	24.0%
Unknown	2	-	1	-	3	-
Age at First Birth						
Nulliparous	84	16.3%	186	13.5%	270	14.3%
< 30	385	74.9%	1060	77.0%	1445	76.4%
30+	43	8.4%	129	9.4%	172	9.1%
Unknown	2	0.4%	2	0.1%	4	0.2%
Menopausal Status						
Pre-Menopausal	107	20.8%	275	20.0%	382	20.2%
Menopausal	397	77.2%	1069	77.6%	1466	77.5%
Unknown	10	1.9%	33	2.4%	43	2.3%
Parous						
Nulliparous	84	16.3%	186	13.5%	270	14.3%
Parous	430	83.7%	1191	86.5%	1621	85.7%
Unknown	0	0.0%	0	0.0%	0	0.0%
Volpara 4 view VBD	514	8.7 (5.3)	1377	7.8 (5.1)	1891	8.1 (5.2)
Volpara 4 view DV	514	66.7 (34.1)	1377	58.5 (28.0)	1891	60.7 (30.0)
V(mean)	510	56.5 (31.2)	1373	50.9 (27.4)	1883	52.4 (28.6)
P_1(mean)	510	18.9 (14.3)	1373	15.6 (14.1)	1883	16.5 (14.2)
p_1(mean)	510	0.3 (0.1)	1373	0.3 (0.1)	1883	0.3 (0.1)

BI-RADS = Breast Imaging Reporting and Data System, BMI = body mass index, VBD = volumetric breast density, DV = dense volume, V=variation, P_1 and p_1 are Fourier measures

Table 2.

Spearman rank correlation (coefficient and 95% confidence intervals) for mammographic measures

Measure	VBD (Volpara)	DV (Volpara)	V	P1	p1
VBD (Volpara)	1.00	0.30 (0.25, 0.34)	0.68 (0.65, 0.71)	0.80 (0.78, 0.82)	0.82 (0.80, 0.84)
DV (Volpara)		1.00	0.48 (0.43, 0.52)	0.33 (0.28, 0.38)	0.31 (0.26, 0.35)
V			1.00	0.74 (0.71, 0.76)	0.68 (0.65, 0.71)
P_1				1.00	0.95 (0.94, 0.95)
p_1					1.00

VBD = volumetric breast density, DV = dense volume, V = variation, P_1 and p_1 are variation measures from restricted regions in the Fourier domain

Table 3.

Association of mammographic measures and breast cancer (514 cases and 1377 controls)

Model		VBD (Volpara)	DV (Volpara)	V	P_1	p_1
a. Continuous Model	**per SD measure**	1.54 (1.33, 1.78)	1.34 (1.20, 1.50)	1.30 (1.16, 1.46)	1.55 (1.35, 1.77)	1.51 (1.33, 1.72)
	Az	0.61 (0.58, 0.64)	0.59 (0.57, 0.62)	0.59 (0.56, 0.61)	0.61 (0.58, 0.63)	0.60 (0.58, 0.63)
b. Quartile Model	**Quartiles of measure**					
	Quartile 1	0.72 (0.52, 1.01)	0.76 (0.55, 1.04)	1.04 (0.74, 1.46)	0.64 (0.46, 0.90)	0.64 (0.46, 0.90)
	Quartile 2	1.00 (REF)	1.00 (REF)	1.00 (REF)	1.00 (REF)	1.00 (REF)
	Quartile 3	1.52 (1.13, 2.05)	1.18 (0.88, 1.58)	1.53 (1.12, 2.10)	1.30 (0.96, 1.74)	1.30 (0.97, 1.76)
	Quartile 4	2.01 (1.43, 2.82)	1.52 (1.13, 2.03)	2.12 (1.54, 2.93)	1.94 (1.41, 2.66)	1.92 (1.40, 2.64)
	Quartile Az	0.60 (0.57, 0.62)	0.58 (0.56, 0.61)	0.59 (0.56, 0.61)	0.60 (0.58, 0.63)	0.60 (0.57, 0.62)
c. Continuous Model + DV Adjustment	**per SD measure**	1.37 (1.14, 1.65)	--	1.13 (0.97, 1.31)	1.43 (1.23, 1.66)	1.40 (1.21, 1.61)
	DV adjustment per SD	1.16 (1.01, 1.33)	--	1.24 (1.08, 1.43)	1.15 (1.02, 1.30)	1.17 (1.03, 1.32)
	Az	0.61 (0.59, 0.64)	--	0.61 (0.58, 0.64)	0.61 (0.58, 0.63)	0.60 (0.58, 0.63)

VBD = volumetric breast density, DV = dense volume, V = variation, SD = standard deviation, Az = characteristic curve, P_1 and p_1= variation measures from restricted regions in the Fourier domain

Table 4.

Mammographic measures and breast cancer associations for the generalization study (1474 cases and 2942 controls)

Model		VBD (Volpara)	DV (Volpara)	V	P_1	p_1
a. Continuous Model	**per SD measure**	1.48 (1.35, 1.62)	1.33 (1.24, 1.43)	1.24 (1.15, 1.34)	1.31 (1.21, 1.43)	1.33 (1.22, 1.45)
	Az	0.59 (0.57, 0.60)	0.58 (0.56, 0.60)	0.56 (0.54, 0.58)	0.57 (0.55, 0.59)	0.58 (0.56, 0.59)
b. Quartile Model	**Quartiles of measure**					
	Quartile 1	0.73 (0.60, 0.89)	0.79 (0.65, 0.96)	0.92 (0.76, 1.12)	0.66 (0.55, 0.81)	0.67 (0.55, 0.82)
	Quartile 2	1.00 (REF)	1.00 (REF)	1.00 (REF)	1.00 (REF)	1.00 (REF)
	Quartile 3	1.44 (1.19, 1.74)	1.23 (1.02, 1.47)	1.44 (1.19, 1.73)	1.18 (0.99, 1.41)	1.22 (1.02, 1.46)
	Quartile 4	1.77 (1.43, 2.18)	1.56 (1.30, 1.87)	1.49 (1.23, 1.80)	1.25 (1.04, 1.51)	1.32 (1.09, 1.61)
	Quartile Az	0.58 (0.56, 0.60)	0.58 (0.56, 0.59)	0.55 (0.54, 0.57)	0.57 (0.55, 0.59)	0.57 (0.55, 0.59)
c. Continuous Model + DV Adjustment	**per SD measure**	1.31 (1.18, 1.46)	--	1.08 (0.99, 1.18)	1.20 (1.10, 1.31)	1.21 (1.11, 1.32)
	DV adjustment per SD	1.18 (1.08, 1.28)	--	1.28 (1.18, 1.39)	1.26 (1.17, 1.36)	1.26 (1.17, 1.36)
	Az	0.59 (0.57, 0.61)	--	0.59 (0.57, 0.60)	0.57 (0.55, 0.59)	0.58 (0.56, 0.60)

VBD = volumetric breast density, DV = dense volume, V = variation, SD = standard deviation, Az = characteristic curve, P_1 and p_1= variation measures from restricted regions in the Fourier domain